The Influence of Horizontal Inhomogeneity on Radiative Characteristics of Clouds: An Asymptotic Case Study

Alexander A. Kokhanovsky

***Abstract*—The paper is devoted to analytical studies of the influence of horizontal inhomogeneity of clouds on their radiative properties in the framework of the asymptotic radiative transfer theory. It is assumed that a cloud field is optically thick. Thus, only overcast cloud fields are under consideration. The study is based on the independent column approximation, assuming Gamma distribution of cloud optical thickness (COT) in the cloud field under study. This paper confirms all essential findings of cloud optics, concerning the influence of horizontally inhomogeneous clouds on transmitted, reflected, and absorbed solar light. For instance, we found the decrease of light reflection and absorption (negative biases) and the increase of light transmission (positive biases) for inhomogeneous clouds as compared to the case of a homogeneous cloud field with the value of optical thickness equal to that of an average COT of an inhomogeneous cloud field. Analytical equations for biases of radiative characteristics (e.g., the reflection function, spherical albedo, transmittance, and absorptance) are derived. Also, for the first time, we established the relationships between biases of different radiative characteristics. Analytical equations proposed are simple and highly accurate for optically thick weakly absorbing cloud fields. They can be incorporated in large-scale atmospheric models for the simplification of radiation blocks both for homogeneous and inhomogeneous cloud fields in visible and near-infrared spectral regions.**

***Index Terms*—Clouds, radiative transfer, remote sensing.**

I. Introduction

The influence of the horizontal inhomogeneity of clouds on their radiative characteristics is a major subject of modern cloud optics studies [3], [6], [7], [9], [10], [12], [25], [26], [38], [43], [44]. In particular, it was found that the horizontal inhomogeneity of clouds effects their abilities to absorb, reflect, and transmit solar light [11], [44]. Thus, cloud remote sensing techniques, based on the spectral reflectance method [1], [14], [18], [22], [32], [33], [40]–[42], should account for the subpixel cloud horizontal inhomogeneity. This is not generally the case so far.

It is known that pixels with inhomogeneous clouds are darker than pixels with homogeneous cloud layers having the same average optical thickness [6]. This leads to the underestimation of cloud optical thickness (COT) by modern satellite retrieval techniques. There are semiempirical approaches to overcome this problem. They are based on the artificial increase of the reflection function measured to account for the horizontal inhomogeneity of a cloud field under study. The correct magnitude of these adjustments, however, cannot be assumed *a priori*. So they lack a physical basis. This issue is discussed in detail by Pincus and Klein [37]. Also cloud inhomogeneity could lead to unphysical dependencies of COT retrieved on illumination and viewing geometry [25].

Another way to solve the problem is to use three-dimensional (3-D) Monte Carlo calculations (e.g., see [44]). However, they are time consuming for realistic clouds and can be used mostly for theoretical studies and not as a core of operational cloud satellite retrieval algorithms. Monte Carlo calculations have shown, however, that in some cases a high accuracy can be achieved if a 3-D cloud field is substituted by N noninteracting vertical columns or cells. A cloud field in each cell is modeled as a horizontally homogeneous plane-parallel layer of an infinite horizontal extent. The optical thickness (and possibly microstructure) of each cell varies, depending on its position in a cloud field. Such an approach is called the independent column approximation (ICA) or the independent pixel approximation (IPA). The range of applicability of the ICA was studied by Davis *et al.* [8] and Schreier and Macke [44].

Effectively, the ICA reduces the 3-D radiative transfer problem to N standard radiative transfer problems for homogeneous media. The number N can be large. Thus, the problem remains computationally very expensive.

It can be simplified, however, if one applies approximate solutions of the radiative transfer problem for each cloud cell. It is done usually in the framework of the two-stream approximation [2]–[4], [36]. However, the accuracy of two-stream approximations [29] is rather low as compared to exact radiative transfer calculations [16], [49]. In particular, for some cases, errors introduced by the approximation can be larger than differences of radiative fluxes for horizontally homogeneous and inhomogeneous cloud fields itself. This approximation also does not allow to consider the bidirectional reflection function of clouds, which is routinely measured by various radiometers and spectrometers on satellite platforms. With this in mind, we propose here to use the asymptotic equations [51] of the radiative transfer theory to solve each of N standard radiative problems, discussed above. Asymptotic formulas are much more accurate than those of the two-stream theory [16]. Typically, the error of asymptotic equations is below 1% for cloud reflection functions with optical thicknesses $\tau \geq 9$ [17].

Manuscript received July 29, 2002; revised December 16, 2002. This work was supported by the Institute of Environmental Physics and Remote Sensing, University of Bremen.

The author is with the Institute of Environmental Physics, University of Bremen, D-28334 Bremen, Germany and also with the Institute of Physics, Minsk 220072, Belarus.

Digital Object Identifier 10.1109/TGRS.2003.811075

The unability to deal with thin clouds is clearly a drawback of the approach presented here. However, the ICA itself is in trouble in this case due to the horizontal photon transport [38]. Moreover, a great portion of clouds has COTs larger than 5–10 [50]. Thus, we believe that results presented here can be used in most of cases, occuring in cloudy atmospheres (and always for overcast conditions).

The main idea behind this paper (apart from the theoretical model proposed) is to quantify the effects of inhomogeneity of clouds on their radiative characteristics in visible and near-infrared spectral ranges, where solar light absorption by clouds is comparatively low.

Our results can be also used in global circulation models (GCMs), which currently entirely neglect the cloud horizontal inhomogeneity [27], [45]. In particular, this drawback leads to inconsistency between the hydrologic and radiative transfer water content treatments in modern GCMs.

II. COT Distribution

It is known that even overcast cloud fields cannot be characterized by a constant geometrical thickness H [3]. Instead, H varies along the cloud field. The same is true for the COT τ and also for other cloud parameters and properties, including their reflection and transmission functions. The statistical theory is, therefore, a natural tool for cloud studies [28].

In this paper, we ignore the variability of cloud microphysical properties (e.g., the size and shape of particles) inside clouds. This allows us to concentrate on the influence of effects of COT variability on cloud reflection and transmission functions. For this, we need to make an assumption on the COT probability distribution function (pdf) $f(\tau)$. Generally speaking, the COT pdf is not a contiuous function, but rather a discrete one. However, for the sake of simplicity it is usually assumed to be a continuous function. Satellite and airborne measurements show that $f(\tau)$ can be well represented by the lognormal, beta, or gamma distribution functions [33], [35]. The gamma distribution is the most convenient for theoretical studies. So, we will use the gamma distribution in this paper. Note, however, that there is a similarity between gamma and log-normal distributions [19]. Also, global optical characteristics of clouds are most sensitive to the average COT

$$\overline{\tau} = \int_0^\infty \tau f(\tau) d\tau \tag{1}$$

and the standard deviation

$$\sigma_\tau = \sqrt{\int_0^\infty (\tau - \overline{\tau})^2 f(\tau) d\tau.} \tag{2}$$

The particular choice of $f(\tau)$, therefore, is of a secondary importance.

Taking into account mentioned above, we assume that

$$f(\tau) = D\tau^\mu \exp\left(-\mu \frac{\tau}{\tau_0}\right) \tag{3}$$

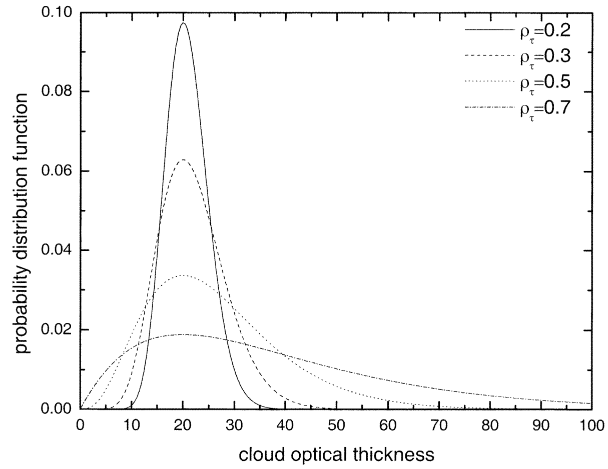

Fig. 1. COT distribution $f(\tau)$ at various values of ρ_τ.

where

$$D = \frac{\mu^{\mu+1}}{\tau_0^{\mu+1}\Gamma(\mu+1)} \tag{4}$$

and $\Gamma(\mu+1)$ is the Gamma function, defined as follows [23]:

$$\Gamma(c) = \int_0^\infty s^{c-1} e^{-s} ds. \tag{5}$$

It holds that

$$\int_0^\infty f(\tau) d\tau = 1. \tag{6}$$

Broken cloud fields, which are out of scope of this paper, can be studied using other approaches (e.g., see Zuev and Titov [53]).

Parameters τ_0 and μ in (3) have a clear meaning. Namely, τ_0 specifies the mode optical thickness, where $f(\tau)$ has a maximum, and μ is the half-width parameter. The distribution is narrower for larger μ.

Let us introduce the coefficient of variance

$$\rho_\tau = \frac{\sigma_\tau}{\overline{\tau}}. \tag{7}$$

The parameter ρ_τ is equal to the ratio standard deviation/mean and has a clear statistical sense. It is often called the inhomogeneity parameter. The pdf (3) is given in Fig. 1 for various values of ρ_τ. We have for the distribution (3)

$$\overline{\tau} = \tau_0 \left(1 + \frac{1}{\mu}\right) \tag{8}$$

$$\rho_\tau = \frac{1}{\sqrt{1+\mu}}. \tag{9}$$

Parameters $\overline{\tau}$ and ρ_τ can be defined for any distribution function $f(\tau)$. Therefore, they are used in the discussion, which follows.

Note that it follows from (8) and (9)

$$\mu = \rho_\tau^{-2} - 1, \tau_0 = (1 - \rho_\tau^2)\overline{\tau}. \tag{10}$$

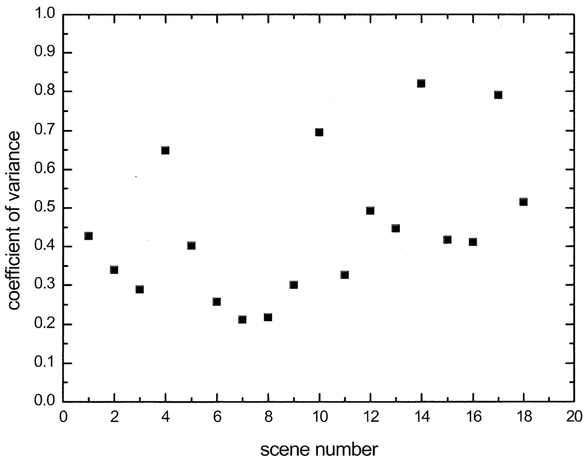

Fig. 2. Values of ρ_τ for various scenes, defined by Barker *et al.* [3].

It follows that $\mu \to \infty$, $\tau_0 \to \overline{\tau}$ as $\rho_\tau \to 0$, as it should be. The value of $\overline{\tau}$ for warm clouds is usually in the range 5–50 [50].

The value of ρ_τ depends on many factors, including the averaging scale. Experimantal data for the value of ρ_τ of natural cloud fields are rare. Nakajima *et al.* [33] found that the value of ρ_τ is in the range of 0.18–0.27 for cloud systems they studied (see Fig. 1). Their functions $f(\tau)$ followed fairly well the log-normal distribution in contrast to highly skewed distributions with long tails for larger τ, reported by Gorodetsky *et al.* [13], King [17], and Heidinger and Stowe [15]. King [17] identified a multimodal nature of the distribution $f(\tau)$ for the cloud system he studied with main modes, located at τ equal to 7, 33, and 45. Our estimation of ρ_τ, obtained from data of Heidinger and Stowe [15] suggests that $\rho_\tau \simeq 0.4$ for their study. Data for ρ_τ, calculated from Barker *et al.* [3, Table II], are presented in Fig. 2. They were obtained analyzing 18 Landsat scenes, having 2048×2048 (scenes 1–5) or 1024×1024 (scenes 6–18) pixels at 28.5- and 57-m resolution, respectively [3]. Pixel values of τ were inferred, using the standard cloud retrieval algorithm for plane-parallel slabs [33]. We see that the value of ρ_τ is in the range 0.2–0.8 for cloud fields studied. The approximate cloud field area Σ was 58×58 km^2 [3] for each scene.

Note that some spectrometers on satellite platforms have the spatial resolution, which is close to (or even larger than) values of Σ reported above.

Thus, it is of importance to study the influence of the parameter ρ_τ on the cloud radiative characteristics. It will be done in this paper assuming that $\rho_\tau = 1/4, 1/3, 1/2$, which cover most of cases presented in Fig. 2 (see also Fig. 1).

It should be pointed out, however, that our study has only a limited value as far as a subpixel cloud inhomogeneity is concerned. Indeed, the current generation of satellite imaging sensors (e.g., see King *et al.* [18] and Nakajima *et al.* [34]) has pixel sizes of 1 km and even less than that, and therefore, the bias ρ_τ is considerably reduced in this case. Also, the horizontal pixel inhomogeneity is of importance for small pixels, which is not accounted for in our model. On the other hand, some modern spectrometers (e.g., [5]) have a large spatial resolution (e.g., 30×60 km^2). Then our analysis is relevant not only in respect to mesoscale cloud properties studies but also for the estimation of influence of subpixel cloud inhomogeneity.

III. Visible Range

A. General Equations

The information on the function $f(\tau)$ allows us to study the optical characteristics of inhomogeneous clouds in the framework of the independent column approximation, which neglects horizontal photon transport. The reflection R and transmission T functions of cloud fields depend on $f(\tau)$. It is not correct to assume that $R(\overline{\tau})$ and $T(\overline{\tau})$ give measured values of reflection and transmission. The relationship-measured signals with the statistical distribution $f(\tau)$ is more involved. Also, the horizontal photon transport can complicate correspondent relationships. For large pixels (e.g., 30×60 km^2), the effects of horizontal photon transport are largely canceled out, and measured values can be well represented by

$$\overline{R} = \int_0^\infty R(\tau) f(\tau) d\tau \tag{11}$$

and

$$\overline{T} = \int_0^\infty T(\tau) f(\tau) d\tau \tag{12}$$

where $f(\tau)$ is the COT pdf. Equations (11) and (12) are of importance not only in subpixel inhomogeneity influence studies (for large pixels), but also in deriving mesoscale cloud radiative properties from measured COT fields $f(\tau)$, which is of importance, for example, for climate change studies.

Other statistical characteristics of random fields $R(\tau)$ and $T(\tau)$, which are determined by the statistical distribution of the COT, can be considered as well, e.g., we have for the coefficient of variance

$$\rho_x = \frac{\sigma_x}{\overline{x}} \tag{13}$$

where

$$\sigma_x = \sqrt{\int_0^\infty (x - \overline{x})^2 f(\tau) d\tau}. \tag{14}$$

Here $x \equiv R, x \equiv T$ or any other relevant cloud radiative characteristic. It is usually assumed in cloud properties retrievals that [14]

$$\overline{x} = x(\overline{\tau}). \tag{15}$$

This relation is correct only in the limit $\rho_x \to 0$ (see Fig. 1). Thus, it is important to study biases

$$B_x = 1 - \frac{x(\overline{\tau})}{\overline{x}} \tag{16}$$

for various cloud radiative characteristics x. This is also of importance for mesoscale cloud radiative characteristics studies.

The main idea of this paper is to study dependencies B_x and ρ_x on $\overline{\tau}$ and ρ_τ for overcast clouds, based on the asymptotic radiative transfer theory valid as $\tau \geq 9$ [17]. We study a large number of cloud characteristics, including the plane albedo, reflection function, cloud absorptance, and cloud transmittance (see Table I). Note that light field polarization characteristics can be considered in a similar way.

TABLE I
DEFINITIONS OF VARIOUS RADIATIVE CHARACTERISTICS [24], [30]. HERE, $T^* = 1/2\pi \int_0^{2\pi} T(\vartheta_0, \vartheta, \varphi) d\varphi$, $R^* = 1/2\pi \int_0^{2\pi} R(\vartheta_0, \vartheta, \varphi) d\varphi$, AND F_0 IS THE INCIDENT FLUX DENSITY. $F^\pm$ IS THE TOTAL OUTGOING FLUX ("+" FOR THE REFLECTED LIGHT FLUX AND "−" OTHERWISE). $I^\pm$ IS THE LIGHT FIELD INTENSITY ("+" FOR THE REFLECTED LIGHT AND "−" OTHERWISE). $\vartheta_0, \vartheta, \varphi$ ARE THE SOLAR ZENITH ANGLE, OBSERVATION ZENITH ANGLE, AND AZIMUTH, RESPECTIVELY

Radiative characterisic	Symbol	Definition
Reflection function	$R(\vartheta_0, \vartheta, \varphi)$	$\frac{\pi I^+}{F_0 \cos \vartheta_0}$
Transmission function	$T(\vartheta_0, \vartheta, \varphi)$	$\frac{\pi I^-}{F_0 \cos \vartheta_0}$
Reflectance (plane albedo)	$R_d(\vartheta_0)$	$\frac{F^+}{F_0 \cos \vartheta_0} = \int_0^{\pi/2} R^*(\vartheta) \sin 2\vartheta d\vartheta$
Diffuse transmittance	$T_d(\vartheta_0)$	$\frac{F^-}{F_0 \cos \vartheta_0} = \int_0^{\pi/2} T^*(\vartheta) \sin 2\vartheta d\vartheta$
Global reflectance (spherical albedo)	r	$\int_0^{\pi/2} R_d(\vartheta_0) \sin 2\vartheta_0 d\vartheta_0$
Global transmittance	t	$\int_0^{\pi/2} T_d(\vartheta_0) \sin 2\vartheta_0 d\vartheta_0$
Absorptance	$A_d(\vartheta_0)$	$1 - R_d(\vartheta_0) - T_d(\vartheta_0)$
Global absorptance	a	$1 - r - t$

TABLE II
MODIFIED ASYMPTOTIC EQUATIONS OF THE RADIATIVE TRANSFER THEORY [20]. HERE, $r_\infty = \exp(-y)$ IS THE SPHERICAL ALBEDO OF A SEMIINFINITE LAYER. $R_{d\infty} = \exp(-yK_0(\vartheta_0))$, $R_\infty(\vartheta_0, \vartheta, \varphi) = R_\infty^0(\vartheta_0, \vartheta, \varphi) \exp(-yu(\vartheta_0, \vartheta, \varphi))$, $u = K_0(\vartheta) K_0(\vartheta_0) / R_\infty^0(\vartheta_0, \vartheta, \varphi)$, $x = \tau\sqrt{3(1-g)(1-\omega_0)}$, $y = 4\sqrt{(1-w_0)/3(1-g)}$, $K_0(\vartheta_0) = (3/7)(1 + 2\cos\vartheta_0)$, $v \approx 1.07$

Radiative characterisic	Symbol	Equation
Reflection function	$R(\vartheta_0, \vartheta, \varphi)$	$R_\infty(\vartheta_0, \vartheta, \varphi) - (r_\infty - r) K_0(\vartheta) K_0(\vartheta_0)$
Transmission function	$T(\vartheta_0, \vartheta, \varphi)$	$tK_0(\vartheta) K_0(\vartheta_0)$
Reflectance (plane albedo)	$R_d(\vartheta_0)$	$R_{d\infty} - (r_\infty - r) K_0(\vartheta_0)$
Transmittance	$T_d(\vartheta_0)$	$tK_0(\vartheta_0)$
Global reflectance (spherical albedo)	r	$\frac{\sinh(x+vy)\exp(-y) - \sinh(y)\exp(-x-y)}{\sinh(x+vy)}$
Global transmittance	t	$\frac{\sinh y}{\sinh(x+vy)}$
Absorptance	$A_d(\vartheta_0)$	$1 - R_d(\vartheta_0) - T_d(\vartheta_0)$
Global absorptance	a	$1 - r - t$

We also consider the relationships between biases of various cloud radiative transfer characteristics (e.g., B_R and B_T, etc.). The general form of such relationships can be easily found, taking into account that a specific directional cloud radiative characteristic x of optically thick cloud fields (e.g., bidirectional reflection function) can be presented as a linear form (see Table II) of the angular averaged value of x, which we denote s

$$x(\tau) = \alpha + \beta s(\tau) \tag{17}$$

where α and β depend on the viewing and illumination geometry (see the Tables I–III), but not on τ. Note that parameters α and β differ for different x (see Tables I–III). It follows from (16) and (17) that

$$B_x = \gamma B_s \tag{18}$$

where

$$\gamma = \frac{\overline{s}}{\overline{s} + \frac{\alpha}{\beta}}. \tag{19}$$

Equations (18) and (19) allow us to reduce the calculation of biases for angular depend characteristics x to the calculation of biases in the values of angular integrated characteristics s, which we can consider as an important result of this study. Numerous specific results of such relationships are given below.

We also note that it follows due to a linearity of (17)

$$\left|\frac{B_x}{B_s}\right| = \frac{\rho_x}{\rho_s}. \tag{20}$$

Therefore

$$\rho_x = |\gamma| \rho_s \tag{21}$$

with the same value of γ as in (18). This means that it is enough to consider the relationship between biases. Relationships between coefficients of variance are similar in form. The difference arises only due to the fact that biases could be negative and positive. By definition, coefficients of variance are positive numbers [see (13)].

Note that $\gamma = 1$ (and therefore $B_x = B_s$ and $\rho_x = \rho_s$) at $\alpha = 0$, which is the case, for example, for transmitted light (see Tables I–III). This means, in particular, that biases for transmission function, diffuse transmittance, and global transmittance coincide in the case of optically thick cloud fields. We consider this point in some detail in Section III-B.

B. Light Transmission

The cloud transmission function does not depend on the azimuth φ for optically thick clouds and is given by the following approximate equation in visible, where light absorption by water droplets can be neglected [21], [51]

$$T(\tau,\xi,\eta) = T_d(\tau)K_0(\eta) \quad T_d(\tau) = t(\tau)K_0(\xi) \tag{22}$$

with a high accuracy. It follows approximately [46]

$$K_0(\xi) = \frac{3}{7}(1+2\xi) \tag{23}$$

and

$$t(\tau) = \frac{1}{0.75\tau(1-g)+\upsilon}. \tag{24}$$

Here $t(\tau)$ is the global transmittance (see Tables I–III). Here $\upsilon \approx 1.07$, $\xi = \cos(\vartheta_0)$, $\eta = \cos(\vartheta)$, ϑ, and ϑ_0 are observation and incidence angles, respectively, and g is the asymmetry parameter of a cloudy medium, which is assumed to be equal to 0.85 throughout this study. The value of $T_d(\tau)$ is called the diffuse transmittance (see Tables I–III). Using results given in Section III-A, we easily obtain

$$\overline{T} = \bar{t}K_0(\xi)K_0(\eta) \tag{25}$$
$$B_T = B_{T_d} = B_t \tag{26}$$
$$\rho_T = \rho_{T_d} = \rho_t. \tag{27}$$

We see, therefore, that the bias of the transmission function B_T (and also the diffuse transmittance bias B_{T_d}) is equal to the bias for the total transmittance B_t. The same is true for coefficients of variance. This is due to the proportionality of functions T and T_d to the value of t and the independence of the function $K_0(\xi)$ on τ.

We have for $\bar{t}$, B_t, and ρ_t [see (12), (13), (16), and (24)] in the case of the Gamma distribution (3)

$$\bar{t} = \upsilon^{-1}z^{\nu}\Psi(\nu,\nu,z) \tag{28}$$
$$B_t = 1 - \frac{1}{(1+\frac{\nu}{z})z^{\nu}\Psi(\nu,\nu,z)} \tag{29}$$
$$\rho_t = \sqrt{\frac{\Psi(\nu,\nu-1,z)}{z^{\nu}\Psi(\nu,\nu,z)} - 1}. \tag{30}$$

Here

$$\Psi(\epsilon,\phi,z) = \frac{1}{\Gamma(\epsilon)}\int_0^{\infty}\frac{\zeta^{\epsilon-1}\exp(-z\zeta)}{(1+\zeta)^{1+\epsilon-\phi}}d\zeta \tag{31}$$

is the confluent hypegeometric function of the second kind [23] and

$$z = \frac{4\nu\upsilon}{3\overline{\tau}(1-g)}, \qquad \nu = 1+\mu = \rho_\tau^{-2}. \tag{32}$$

We see, therefore, that values of $\bar{t}$, B_t, and ρ_t are determined by two parameters, namely ν and z, which are related to ρ_τ and $\overline{\tau}$. Using the asymptotical behavior of the function $\Psi(\epsilon,\phi,z)$ at small z, we obtain as $\overline{\tau} \to \infty$

$$\bar{t} = \frac{4}{3\overline{\tau}(1-g)(1-\rho_\tau^2)} \tag{33}$$
$$B_t = \rho_\tau^2 \tag{34}$$
$$\rho_t = \frac{\rho_\tau}{\sqrt{1-2\rho_\tau^2}}. \tag{35}$$

Therefore, the problem of finding biases for the transmission function T and the diffused transmittance T_d is reduced in the case studied to the same problem but for the global transmittance t. This allows to avoid geometric considerations (e.g., the account for angles ϑ_0, ϑ, and φ). Also, it means that biases in the transmission T are angular independent. They are determined only by values $\overline{\tau}$ and ρ_τ in the Gamma-independent column approximation studied here.

Functions $B_t(\overline{\tau})$ and $\rho_t(\overline{\tau})$, obtained from (29) and (30), are presented in Fig. 3(a) and (b) at $\rho_\tau = 1/4, 1/3, 1/2$. We see that both $B_t(\overline{\tau})$ and $\rho_t\ (\overline{\tau})$ increase with $\overline{\tau}$. They tend to asymptotic limits, given by (34) and (35), respectively, as $\overline{\tau} \to \infty$.

The bias B_t is positive. It means that $t(\overline{\tau}) < \bar{t}$ [see (16)]. One concludes from Fig. 3(a) that B_t can reach 20% at $\overline{\tau} = 100$ and $\rho_\tau = 0.5$, which is not a small number as far as climate change and cloud remote sensing algorithms are of concern.

C. Light Reflection

Let us consider now quantities (11), (13), and (16) for the reflected light. For this we note that the reflection function of optically thick clouds is given by the following expression in the visible, where light absorption by clouds can be often neglected [20], [51], [52]:

$$R(\xi,\eta,\varphi,\tau) = R_\infty^0(\xi,\eta,\varphi) - t(\tau)K_0(\xi)K_0(\eta). \tag{36}$$

By definition, $R_\infty^0(\xi,\eta,\varphi) = R(\xi,\eta,\varphi,\tau \to \infty)$ does not depend on τ. So we have taking into account results given in Section III-A

$$\overline{R}(\xi,\eta,\varphi,\tau) = R_\infty^0(\xi,\eta,\varphi)(1-u\bar{t}) \tag{37}$$
$$B_R = -MB_t \tag{38}$$
$$\rho_R = |M|\rho_t \tag{39}$$

where

$$M = \frac{u\bar{t}}{1-u\bar{t}} \tag{40}$$
$$u = \frac{K_0(\xi)K_0(\eta)}{R_\infty^0(\xi,\eta,\varphi)}. \tag{41}$$

We see, therefore, that the problem of finding biases for the reflection function is reduced to the problem studied in Section III-B. So, having information on $\bar{t}$, B_t, and ρ_t, one can easily derive $\overline{R}$, B_R, and ρ_R. For this, also, we need to know the function $R_\infty^0(\xi,\eta,\varphi) = R(\xi,\eta,\varphi,\tau \to \infty)$ (e.g., see [31]).

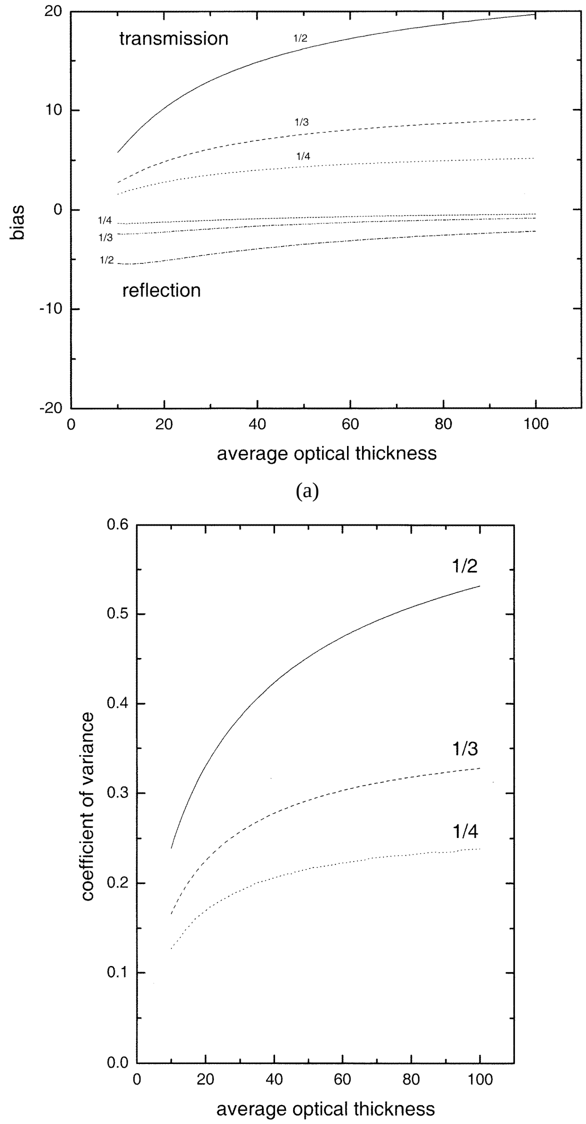

(a)

(b)

Fig. 3. (a) Dependencies $B_t(\overline{\tau}) > 0$, $B_r(\overline{\tau}) < 0$ (in percent) at $\rho_\tau = 1/4$, 1/3, 1/2. (b) The dependence $\rho_t(\overline{\tau})$ at $\rho_\tau = 1/4$, 1/3, 1/2.

This function practically does not depend on the cloud microphysical parameters and can be considered as a universal function in most of cases [19], [20].

We present the amplification coefficient M, given by (40), in Fig. 4. It increases from 0 to 1.5 while $b = u\overline{t}$ changes from 0 to 0.6. For optically thick clouds, $\overline{t}$ is usually a small number, and $M < 1$, which means that B_R and ρ_R are smaller than B_T and ρ_T, respectively. Clearly, for semiinfinite clouds, we have $B_R \equiv 0$ and $\rho_R \equiv 0$.

The function $u(\vartheta_0)$ at nadir observation [see (41)] is given in Fig. 5, where we used the analytical expression for $R^0_\infty(\vartheta_0, \vartheta = 0)$, given by Kokhanovsky [20]. The value of u [and therefore M; see (40)] generally decreases with the solar zenith angle. Thus, low sun will lead to smaller values of $|B_R|$ and ρ_R [see (38) and (39)]. This can produce unphysical dependencies $\tau(\vartheta_0)$ in operational cloud retrieval algorithms.

We see that $M > 0$. This means that biases for reflection and transmission have different signs. They are positive for the transmission, but negative for the reflection. Inhomogeneous clouds, therefore, reflect smaller amount of light as compared to homogeneous clouds with the value of $\tau = \overline{\tau}$. The opposite is true for the transmission, which increases for inhomogeneous cloud fields [52].

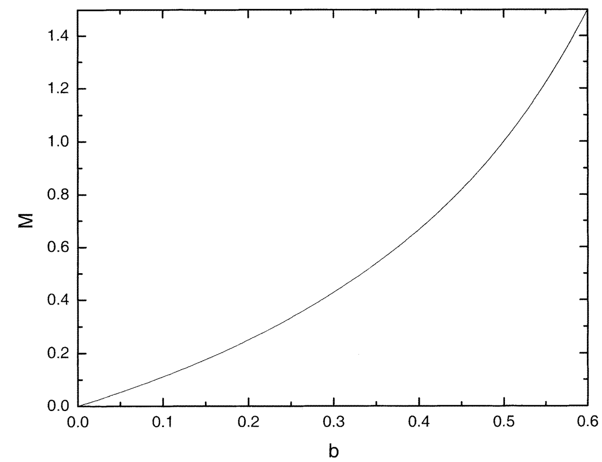

Fig. 4. Dependence of the amplification coefficient M on the parameter $b = u\overline{t}$ [see (40)].

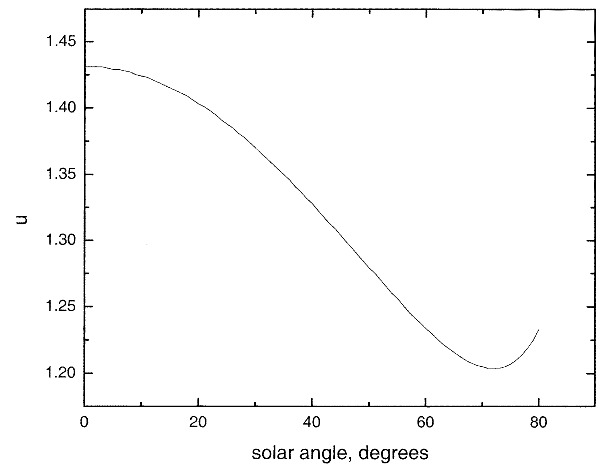

Fig. 5. Dependence $u(\vartheta_0)$, obtained from (41).

The dependencies $B_R(\overline{\tau})$ and $\rho_R(\overline{\tau})$ at $\rho_\tau = 1/4, 1/3, 1/2$, obtained from (38) and (39), are given in Figs. 6 and 7 ($\vartheta_0 = 60^\circ$, $\vartheta = 0^\circ$). As expected, $|B_R|$ decreases with $\overline{\tau}$. It increases with ρ_τ. However, the bias is not negligable for smaller $\overline{\tau}$, e.g., it is 8.5% at $\overline{\tau} = 10$ and $\rho_\tau = 0.5$ (see Fig. 6). Such biases cannot be ignored in satellite cloud retrival algorithms, based on the passive remote sensing techniques.

Let us briefly consider the case of the diffuse reflectance and spherical albedo (see Tables I–III). Then we have

$$\overline{R}_d(\xi) = 1 - \overline{t}K_0(\xi) \tag{42}$$

$$B_{R_d} = -NB_t \tag{43}$$

$$\rho_R = |N|\,\rho_t \tag{44}$$

where

$$N = \frac{K_0(\xi)\overline{t}}{1 - K_0(\xi)\overline{t}}. \tag{45}$$

Here we accounted for the fact that $R_{d\infty}$ and r_∞ (see Table III) are both equal to one for nonabsorbing media [19]. We see again

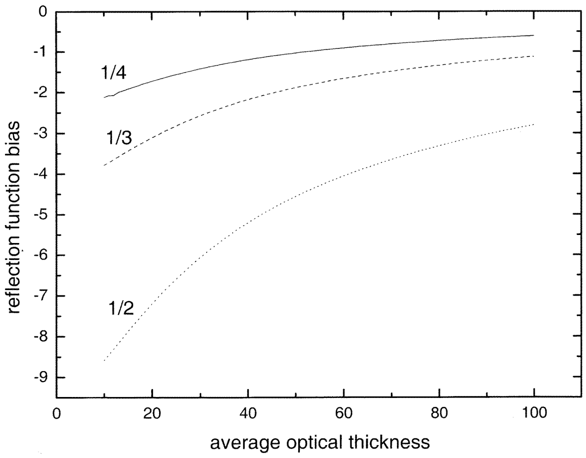

Fig. 6. Dependence $B_R(\overline{\tau})$ (in percent) at $\vartheta_0 = 60°$, $\vartheta = 0°$.

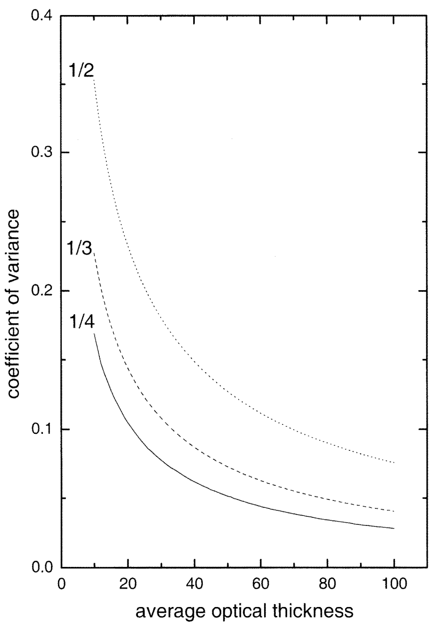

Fig. 7. Dependence $\rho_R(\overline{\tau})$ (in percent) at $\vartheta_0 = 60°$, $\vartheta = 0°$.

TABLE III
AVERAGE RADIATIVE CHARACTERISTICS ($A_{d\infty} = 1 - R_{d\infty}, a_\infty = 1 - r_\infty$)

$\overline{R} =$	$R_\infty - (r_\infty - \overline{r})\, K_0(\vartheta)\, K_0(\vartheta_0)$
$\overline{R_d} =$	$R_{d\infty} - (r_\infty - \overline{r})\, K_0(\vartheta_0)$
$\overline{T} =$	$\overline{t} K_0(\vartheta)\, K_0(\vartheta_0)$
$\overline{T_d} =$	$\overline{t} K_0(\vartheta_0)$
$\overline{A_d} =$	$A_{d\infty} + (\overline{a} - a_\infty)\, K_0(\vartheta_0)$
$\overline{a} =$	$1 - \overline{r} - \overline{t}$

that the multiplier $N > 0$ as in the case of reflection function. It follows for the spherical albedo $\overline{r}$ and values B_r and ρ_r (see Tables I–III)

$$\overline{r} = 1 - \overline{t} \quad B_r = -LB_t \quad \rho_r = L\rho_t \tag{46}$$

where

$$L = \frac{\overline{t}}{1 - \overline{t}}. \tag{47}$$

The dependence $B_r(\overline{\tau})$ is given in Fig. 3(a). We see that it is negative and $|B_r| < |B_t|$. Thus, effects of clouds inhomogeneity are more important in the transmission than in the reflection for a special case of overcast cloud fields considered here.

We undeline once more that biases of different radiative characteristics are not independent. The analytical relationships between them are given above.

IV. Near-Infrared Range

Let us consider now the near-infrared range, where cloud particles absorb incident solar light. The exact asymptotic theory leads to quite complex expressions for reflection and transmission functions, if the value of the single scattering albedo ω_0 is arbitrary [51]. However, ω_0 is close to one for clouds in the near-infrared region of the electromagnetic spectrum [19]. It allows to substitute exact asymptotic formulas by more simple relations almost not loosing the accuracy [20], [52]. These relations will be used in this section to consider the case of absorbing inhomogeneous clouds. They are given in Table II. Correspondent equations for various average radiative transfer characteristics are presented in Table III.

We see that radiative transfer characteristics of inhomogeneous clouds depend on R_∞, r_∞, $\overline{r}$, $\overline{t}$, and $K_0(\vartheta_0)$. Functions $R_\infty, K_0(\vartheta_0)$, and r_∞ are given in Tables I–III and

$$\overline{r} = \int_0^\infty r(\tau) f(\tau) d\tau \quad \overline{t} = \int_0^\infty t(\tau) f(\tau) d\tau \tag{48}$$

where [20]

$$r(\tau) = \frac{\sinh(x + \upsilon y)\exp(-y) - \sinh(y)\exp(-x - y)}{\sinh(x + \upsilon y)} \tag{49}$$

and

$$t(\tau) = \frac{\sinh y}{\sinh(x + \upsilon y)}. \tag{50}$$

Here $\upsilon \approx 1.07$ as specified above and

$$x = \tau\sqrt{3(1-g)(1-\omega_0)} \quad y = 4\sqrt{\frac{(1-\omega_0)}{3(1-g)}}. \tag{51}$$

It is easy to show in a full anology with results obtained above that

$$B_R = PB_r \quad B_{R_d} = QB_r \quad B_T = B_{T_d} = B_t \tag{52}$$

where

$$P = \frac{\overline{r}u}{1 - (r_\infty - \overline{r})u} \quad Q = \frac{\overline{r}K_0(\vartheta_0)}{1 - (r_\infty - \overline{r})K_0(\vartheta_0)}. \tag{53}$$

Expressions similar in form hold for coefficients of variance [see (21)].

Let us introduce also the absorption function $A = 1 - R - T$, the absorptance $A_d = 1 - R_d - T_d$, and the global absorptance $a = 1 - r - t$. The value of A_d gives a fraction of solar energy absorbed by a cloud field for a given sun zenith angle. Then we have

$$\overline{A} = 1 - \overline{R} - \overline{T} \quad \overline{A}_d = 1 - \overline{R}_d - \overline{R}_d \quad \overline{a} = 1 - \overline{r} - \overline{t} \tag{54}$$

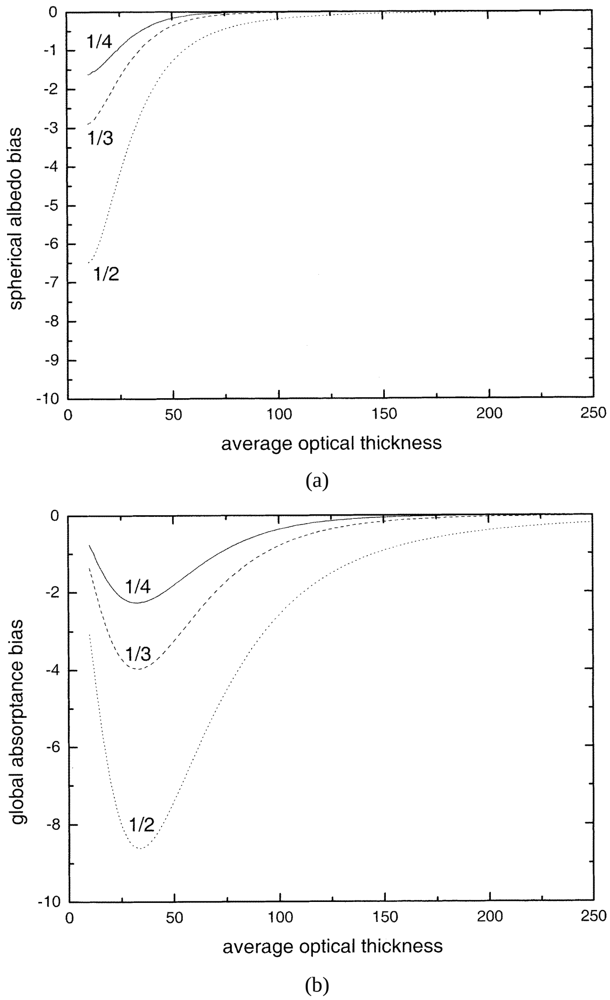

Fig. 8. (a) Dependence $B_r(\overline{\tau})$ (in percent) at the probability of photon absorption $\beta = 0.01$, the asymmetry parameter $g = 0.85$, and $\rho_\tau = 1/4$, $1/3$, $1/2$. (b) Dependence $B_a(\overline{\tau})$ (in percent) for the same conditions as in (a).

and

$$B_A = VB_a \quad B_{A_d} = WB_a \tag{55}$$

where [see (19)]

$$V = \frac{\overline{a}}{\overline{a} + \Xi} \quad W = \frac{\overline{a}}{\overline{a} + \Theta}. \tag{56}$$

Here

$$\Xi = \frac{1 - R_\infty - a_\infty K_0(\xi)K_0(\eta)}{K_0(\xi)K_0(\eta)},$$
$$\Theta = \frac{1 - R_{d\infty} - a_\infty K_0(\xi)}{K_0(\xi)} \tag{57}$$

and $a_\infty = 1 - r_\infty$.

Thus, the biases B_R, B_T, B_A, and correspondent coefficients of variance ρ_R, ρ_T, and ρ_A are easily obtained if the values of B_r, B_t, B_a, ρ_r, ρ_t, and ρ_a for absorbing inhomogeneous clouds are known.

The results of the numerical calculation of values B_r and B_a using (16) and formulas given in the Tables I–III for absorbing clouds are presented in Fig. 8(a) and (b). It was assumed that $\beta = 1 - \omega_0 = 0.01$ and $g = 0.85$. It follows that $|B_r|$ decreases with $\overline{\tau}$ and $B_r < 0$. This corresponds to similar results given in Fig. 3(a) for nonabsorbing clouds. The dependence $|B_a(\overline{\tau})|$ has a maximum, which is located approximately at $\overline{\tau} = 30$ for the case studied. The fact that $B_a(\overline{\tau}) < 0$ points out that inhomogeneity of clouds leads to the decrease of the cloud absorption as compared to the case of homogeneous clouds with the same average optical thickness ($\overline{a} < a(\overline{\tau})$).

V. Conclusion

The study of the influence of the horizontal inhomogeneity on cloud radiative characteristics are usually performed using Monte Carlo techniques, which are computationally very expensive. They are related only to the specific cases computed. Other approaches (e.g., the two-flux approximation) are characterized by a poor accuracy and are limited to the calculation of light fluxes.

In this paper, we propose the use of the asymptotic equations of the radiative transfer theory, which are valid at $\tau > 9$, in combination with the independent column approximation to study the influence of the horizontal inhomogeneity on the radiative properties of overcast cloudiness.

Final formulas (e.g., see Tables I–III) are simple and allow for a rapid estimation of cloud inhomogeneity effects in the asymptotic limit of large τ. In particular, we confirm that cloud inhomogeneity leads to the increase of transmission and the decrease of reflection and absorption as compared to the case of homogeneous clouds with the same average optical thickness. This may complicate so-called cloud absorption paradox [39], [47], [48] and have an importance for climatological studies.

We find that biases for all radiative characteristics studied can be expressed via the bias B_t (or B_r) in the case of nonabsorbing (e.g., in the visible range) optically thick clouds. For absorbing clouds (e.g., in the near-infrared range), we have established relationships between biases of angular integrated and directional quintities.

The procedure for calculation of averages given here can be used to improve radiation blocks in modern global circulation models for the case of overcast cloud fields.

Acknowledgment

This work is a part of preparation for the interpretation of data from Scanning Imaging Absorption Spectrometer for Atmospheric Chartography (SCIAMACHY) onboard the ENVIronmental SATellite (ENVISAT) taken over overcast cloud fields. The author is grateful to A. Davis, A. Macke, B. Mayer, and V. V. Rozanov for help and discussions related to light transport in 3-D random media.

References

[1] A. Arking and J. D. Childs, “Retrieval of clouds cover parameters from multispectral satellite images,” *J. Appl. Meteorol.*, vol. 24, pp. 323–333, 1985.

[2] H. W. Barker, “A parametrization for comparing grid-averaged solar fluxes for marine boundary layer clouds. Part I: Methodology and honogeneous biases,” *J. Atmos. Sci.*, vol. 53, pp. 2289–2303, 1996.

[3] H. W. Barker *et al.*, “A parametrization for computing grid-averaged solar fluxes for inhomogeneous marine boundary layer clouds, II, validation using satellite data,” *J. Atmos. Sci.*, vol. 53, pp. 2304–2316, 1996.

[4] H. W. Barker and Q. Fu, “Assesment and optimization of the gamma-weighted two-stream approximation,” *J. Atmos.*, vol. 57, pp. 1181–1188, 2001.

[5] H. Bovensmann *et al.*, "SCIAMACHY: Mission objectives and measurement modes," *J. Atmos. Sci.*, vol. 56, pp. 127–150, 1999.
[6] R. F. Cahalan *et al.*, "The albedo of fractal stratocumulus clouds," *J. Atmos. Sci.*, vol. 51, pp. 2434–2455, 1994.
[7] ——, "Cloud characterization and clear-sky correction from Landsat-7," *Remote Sens. Environ.*, vol. 78, pp. 83–98, 2001.
[8] A. Davis *et al.*, "The Landsat scale break in stratocumulus as a three-dimensional radiative transfer effect: Implications for cloud remote sensing," *J. Atmos. Sci.*, vol. 54, pp. 241–260, 1997.
[9] A. Davis and A. Marshak, "Space-time characteristics of light transmitted through dense clouds: A Green's function analysis," *J. Atmos. Sci.*, vol. 59, pp. 2713–2727, 2002.
[10] D. P. Duda *et al.*, "Effects of aerosol and horizontal inhomogeneity on the broadband albedo of marine stratus: Numerical simulations," *J. Atmos. Sci.*, vol. 53, pp. 3757–3769, 1996.
[11] E. M. Feigelson, Ed., *Radiation in a Cloudy Atmosphere*. Leningrad, Russia: Gidrometeoizdat, 1981, p. 280.
[12] Q. Fu *et al.*, "Cirrus horizontal inhomogeneity and OLR bias," *Geophys. Res. Lett.*, vol. 27, pp. 3341–3344, 2000.
[13] A. K. Gorodetsky *et al.*, "Light scattering coefficients in layered clouds," *Izv. Acad. Sci. USSR Atmos. Ocean. Phys.*, vol. 16, pp. 494–499, 1980.
[14] Q. Han *et al.*, "Near global survey of effective droplet radii in liquid water clouds using ISCCP data," *J. Climate*, vol. 7, pp. 465–497, 1994.
[15] A. K. Heidinger and L. L. Stowe, "Cloud optical property retrievals from layered-cloud radiances from AVHRR data," in *SIPIE Proc. EUROPTO Conf. Satellite Remote Sensing of Clouds and the Atmosphere III*, vol. 3495, 1998, pp. 12–16.
[16] M. D. King and Harshvarhan, "Comparative accuracy of selected multiple scattering approxiamtion," *J. Atmos. Sci.*, vol. 43, pp. 784–801, 1986.
[17] M. D. King, "Determination of the scaled optical thickness of clouds from reflected solar radiation measurements," *J. Atmos. Sci.*, vol. 44, pp. 1734–1751, 1987.
[18] M. D. King *et al.*, "Remote sensing of cloud, aerosol, and water vapor properties from the Moderate Resolution Imaging Spectrometer (MODIS)," *IEEE Trans. Geosci. Remote Sensing*, vol. 30, pp. 2–27, Jan. 1992.
[19] A. A. Kokhanovsky, *Light Scattering Media Optics: Problems and Solutions*. Chichester, U.K.: Praxis-Springer, 2001.
[20] ——, "Simple approximate formula for the reflection function of a homogeneous semi-infinite turbid medium," *J. Opt. Soc. Amer.*, vol. A19, pp. 957–960, 2002.
[21] A. A. Kokhanovsky *et al.*, "The semi-analytical cloud retrieval algorithm, based on measurements of backscattered light in the region 0.4–2.4 μm," *J. Geophys. D*, vol. 108, 2003.
[22] K. Y. Kondratyev and V. I. Binenko, *Impact of Cloudiness on Radiation and Climate*. Leningrad, Russia: Gidrometeoizdat, 1984.
[23] N. N. Lebedev, *Special Functions and Their Applications*. Upper Saddle River, NJ: Prentice-Hall, 1965.
[24] K. N. Liou, *Radiation and Cloud Processes in the Atmosphere*. Oxford, U.K.: Oxford Univ. Press, 1992.
[25] N. G. Loeb and R. Davies, "Observational evidence of plane parallel model biases: Apparent dependence of cloud optical depth on solar zenith angle," *J. Geophys. Res.*, vol. 101, pp. 1621–1634, 1996.
[26] A. Marshak *et al.*, "Nonlocal independent pixel approximation: Direct and inverse problems," *IEEE Trans. Geosci. Remote Sensing*, vol. 36, pp. 192–205, Jan. 1998.
[27] N. A. McFarlane *et al.*, "The Canadian Climate Centre second-generation circulation model and its equilibrium climate," *J. Climate*, vol. 5, pp. 1013–1044, 1992.
[28] D. McKague and K. F. Evans, "Multichannel satellite retrieval of cloud parameter probability distribution functions," *J. Atmos. Sci.*, vol. 59, pp. 1371–1382, 2002.
[29] W. E. Meador and W. R. Weaver, "Two-stream approximations to radiative transfer in planetary atmospheres: A unified description of existing methods and a new improvement," *J. Atmos. Sci.*, vol. 37, pp. 630–643, 1980.
[30] I. N. Minin, *Radiative Transfer Theory in Planetary Atmospheres*. Moscow, Russia: Nauka, 1988.
[31] M. I. Mishchenko *et al.*, "Bidirectional reflection of flat, optically thick particulate layers: An efficient radiative transfer solution and applications to snow and soil surfaces," *J. Quant. Spectros. Rad. Transf.*, vol. 63, pp. 409–432, 1999.
[32] T. Nakajima and M. D. King, "Determination of the optical thickness and effective particle radius of clouds from reflected solar radiation measurements," *J. Atmos. Sci.*, vol. 47, pp. 1878–1893, 1990.
[33] T. Nakajima *et al.*, "Determination of the optical thickness and effective particle radius of clouds from reflected solar radiation measurements. Part II. Marine stratocumulus observations," *J. Atmos. Sci.*, vol. 48, pp. 728–750, 1991.
[34] T. Y. Nakajima *et al.*, "Optimization of advanced earth observing satellite II global imager channels by use of the radiative transfer calculations," *Appl. Opt.*, vol. 37, pp. 3149–3163, 1998.
[35] L. Oreopoulos and R. Davies, "Plane parallel albedo biases from satellite observations. Part II: Parametrization for bias removal," *J. Climate*, vol. 11, pp. 933–944, 1998.
[36] L. Oreopoulos and H. W. Barker, "Accounting for subgrid-scale cloud variability in a multi-layer, 1D solar radiative transfer algorithm," *Q. J. R. Meteorol. Soc.*, vol. 125, pp. 301–330, 1999.
[37] R. Pincus and S. Klein, "Unresolved spatial variability and microphysical process rates in large-scale models," *J. Geophys. Res.*, vol. 105, no. D22, pp. 27 059–27 065, 2000.
[38] S. Platnick, "Approximations for horizontal photon transport in cloud remote sensing problems," *J. Quant. Spectros. Rad. Transf.*, vol. 68, pp. 75–99, 2001.
[39] P. Pilewskie and F. P. J. Valero, "Direct observation of excess solar absorption by clouds," *Science*, vol. 267, pp. 1626–1629, 1995.
[40] W. B. Rossow, L. C. Garder, and A. A. Lacis, "Global, seasonal cloud variations from satellite radiance measurements. Part I: Sensitivity of analysis," *J. Climate*, vol. 2, pp. 419–458, 1989.
[41] W. B. Rossow and R. A. Schiffer, "Advances in understanding clouds from ISCCP," *Bull. Amer. Meteorol. Soc.*, vol. 80, pp. 2261–2287, 1999.
[42] G. V. Rozenberg *et al.*, "Determination of optical characteristics of clouds from measurements of reflected solar radiation on the Kosmos 320 satellite," *Izv. Acad. Sci. USSR Atmos. Ocean. Phys.*, vol. 10, pp. 14–24, 1974.
[43] R. Schreier, "Solarer Stralungstransport in der inhomogenen Atmosphare," Ph.D. thesis, Inst. fur Meereskunde, 2001.
[44] R. Schreier and A. Macke, "On the accuracy of the independent column approximation in calculating the downward fluxes in the UVA, UVB, and PAR spectral regions," *J. Geophys. Res.*, vol. 106, no. D13, pp. 14 301–14 312, 2001.
[45] A. Slingo, "A GCM parameterization for the shortwave radiative properties of water clouds," *J. Atmos. Sci.*, vol. 46, pp. 1419–1427, 1989.
[46] V. V. Sobolev, *Light Scattering in Planetary Atmospheres*. Moscow, Russia: Nauka, 1972.
[47] G. L. Stephens and S. C. Tsay, "On the cloud absorption anomaly," *Q. J. R. Meteorol. Soc.*, vol. 116, pp. 671–689, 1990.
[48] G. L. Stephens, "How much solar radiation do clouds absorb," *Science*, vol. 271, pp. 1131–1136, 1996.
[49] G. E. Thomas and K. Stamnes, *Radiative Transfer in the Atmosphere and Ocean*. Cambridge, U.K.: Cambridge Univ. Press, 1999.
[50] A. P. Trishchenko *et al.*, "Cloud optical depth and TOA fluxes: Comparison between satellite and surface retrievals from multiple platforms," *Geophys. Res. Lett.*, vol. 28, pp. 979–982, 2001.
[51] H. C. van de Hulst, *Multiple Light Scattering*. New York: Academic Press, 1980.
[52] E. P. Zege, A. P. Ivanov, and I. L. Katsev, *Image Transfer through a Scattering Medium*. New York: Springer-Verlag, 1991.
[53] V. E. Zuev and G. A. Titov, *Atmospheric Optics and Climate*: Inst. Atmospheric Optics, 1996.

Alexander A. Kokhanovsky received the B.A. and M.S. degrees in theoretical physics from the Belarussian State University, Minsk, Belarus, in 1983, and the M.S. and Ph.D. degrees in optical sciences from the B. I. Stepanov Institute of Physics, National Academy of Sciences of Belarus, Minsk, Belarus, in 1991.

He is currently a member of the SCIAMACHY/ ENVISAT algorithm development team at the Institute of Environmental Physics, University of Bremen, Bremen, Germany. He has been with the Laboratory of Light Scattering Media Optics, B. I. Stepanov Institute of Physics since 1983. His research interests are directed toward modeling light propagation and scattering in terrestrial atmosphere. He is the author of *Light Scattering Media Optics: Problems and Solutions* (Chichester, U.K.: Springer-Praxis, 2001) and *Polarization Optics of Random Media* (Berlin, Germany: Springer-Praxis, 2003).

Dr. Kokhanovsky is a member of the American Geophysical Union and the Belarussian Physical Society.